RSC Advances

ROYAL SOCIETY OF CHEMISTRY

www.rsc.org/advances

Selective complexation of alkaline earth metal ions with nanotubular cyclopeptides: DFT theoretical study

Fereshte Shahangi[a], Alireza Najafi Chermahini*[a], Hossein Farrokhpour[a], Abbas Teimouri[b]

[a] *Department of Chemistry, Isfahan University of Technology, Isfahan 84156-83111, Iran, email:anajafi@cc.iut.ac.ir, Tel: +983113913251, Fax:+983113913250*

[b] *Chemistry Department, Payame Noor University, 19395-4697 Tehran, Iran*

ABSTRACT

The interaction of alkaline earth metal cations including Be^{2+}, Mg^{2+}, Ca^{2+}, Sr^{2+} and Ba^{2+} with cyclic peptides containing 3 or 4 (*S*) alanine molecules (**CyAla3** and **CyAla4**) was investigated by density functional theory (DFT-CAM-B3LYP and DFT-B3LYP). A mixed basis set including 6-31+G(d) for C, H, O, Be^{2+}, Mg^{2+}, Ca^{2+} and LANL2DZ for Sr^{2+} and Ba^{2+} were used for calculations. The optimized structures, binding energies, and various thermodynamic parameters of free ligands and related metal cation complexes were determined. The order of strength of interaction energies was found as $Be^{2+} > Mg^{2+} > Ca^{2+} > Sr^{2+} > Ba^{2+}$. Vibrational frequency calculations showed that the selected cyclic peptides and their complexes with the alkaline earth metal cations were at local minima of their potential energy surfaces. In addition, it was found that the larger cavity **CyAla4** ligand, can hold the alkaline metal cations better than **CyAla3** molecule when the same metal cation is in the structure of complex**.** Moreover, analyzing the geometry of $[\mathbf{M/CyAla3}]^{2+}$ and $[\mathbf{M/CyAla4}]^{2+}$ complexes indicated that the aggregation with metal cation, caused substantial changes in the geometrical parameters of ligands.

Keywords: Host-guest complex; DFT, CAM-B3LYP; Nanotubular cyclic peptides; Cation selectivity; Alkaline earth metals.

1. Introduction

Supramolecular chemistry appeared when the Nobel Prize was awarded by Charles J Pedersen, Donald J Cram and Jean-Marie Lehn in 1987. Lehn specified supramolecular chemistry as 'chemistry beyond the molecule', i.e. the chemistry of molecular aggregates assembled via non-covalent interactions. [1] After two decades, supramolecular chemistry is an essential, knowledge base branch of science encompassing opinions of physical and biological processes. Host-Guest chemistry is an example of supramolecular chemistry. It is the study of complexes that are composed of molecules or ions held together by intermolecular forces, such as electrostatic interactions, hydrogen bonding, and dispersion interactions, and solvophobic effects not by covalent bonds. [2] The discovery of crown ethers is the milestone for starting the extensive evolution of host-guest chemistry in 1967. [3] Shortly afterwards,various classes of macrocyclic ligands with structures of increasing complexity were synthesized, including cryptands, [4] cavitands, [5] carcerands, [6] cyclodextrins (CDs), [7, 8] macrocyclic antibiotics, [9, 10] proteins [11] and chiral micelles. [12] In the host-guest chemistry an inclusion compound is a complex in which one chemical compound ("host") forms an enclosed space in which molecules of a second "guest" compound are situated.[13, 14] There are various experimental [15-17] and theoretical [18-22] studies devoted to investigate different aspects of this phenomenon. The definition of inclusion compounds is very broad: for example in molecular encapsulation a guest molecule is actually trapped inside another molecule. [23]

In recent years, a new fascinating class of organic compounds has been reported in which amino acid unites make a macrocycle named cyclic peptide. [24-28] Cyclic peptides have been defined in many natural environments and display a wide spectrum of biological activity. [29] For example they have antibacterial, [30] antiviral, [31] antifungal, [32] immunosuppressant, [33] and

antinociceptive properties. [34] Their amphiphilic characteristics make them to be potential superior candidates of surfactants. [35] Also, cyclic peptides can self-assemble into peptide nanotubes, as models of biological transmembrane channels.[36, 37] Such surfaces and their biological properties have attracted interest in the structures of cyclic peptides and their behaviors at the hydrophilic/hydrophobic interfaces. The structure and properties of cyclic peptides have been deeply studied and results reported in literature. Chen and co-workers have studied characteristics of cyclic peptides based on the density function theory (DFT-B3LYP) and examined the effect of the substituents and ring size on molecular structure of cyclic peptides. [24] Poteau and Trinquier investigated the structures of all-cis cyclopolyglycines, cis cyclopolyalanines and cyclopolyphenylalanines based on theoretical approaches. [28] Vijayaraj et al. reported structures and geometries of cyclic peptide nanotubes by molecular dynamic simulations. [38, 39] Mazurek and co workers studied structures and properties of cyclo glycine and compared these with its phosphor analogues. [40] In addition, Jishi et al. investigated formation of dimers of Cyclo[(Gly-D-Ala)4] and concluded that dimer formation is favored by hydrogen bonding. [41] Hongge Zhao and co-workers used a cyclic decapeptide and the enantiomers of 1-phenyl-1-propanol as the host and guest molecules, respectively, to examine the separation ability of guest enantiomers by the cyclic peptide. [42] Collision-induced dissociation (CID) of protonated peptides are the most frequently practiced MS/MS technology in proteomics. [43-45] In collision-induced dissociation of a peptide, cleavage of an amide bond can result in namely b fragment ion with a five-membered oxazolone ring on the C-terminal side as first postulated by Harrison .[46, 47] These oxazolone structures can isomerize to macrocyclic peptides via a head to tail nucleophilic attack from the N-terminus.

The interaction of metal cations with cyclic peptides has been subjected of various studies especially for obtaining sequence information . [48-58] For example Williams and Brodbelt used low energy collisionally activated dissociation (CAD) in a quadrupole ion trap were used to characterize the fragmentation of alkali, alkaline earth and transition metal complexes of five cyclic peptides .[48] Moreover, Zhang et.al studied the interaction of disulfide-constrained cyclic tetrapeptides with Cu^{2+}.[57]In addition, Ruotolo and co-workers performed a conformational analysis of Gramicidin S, a cyclic antimicrobial peptide and found a β-sheet conformational preference .[52]

Recently, we have investigated the ability of cyclo alanines with different sizes for separating lactic acid enantiomers and metal alkali cations. [59,60] Our previous theoretical calculations have pointed that **CyAla3** and **CyAla4** cyclic peptides are appropriate ligands for the separation of Li^+ and Na^+ from other alkali metal ions. Additionally, the binding energy of Li^+ is greater than Na^+ metal ion due to the smaller size of the Li^+ ion. In continuum with our previous studies, our aim in this work is to employ the DFT approach along with a suitable basis set, to examine the influence of the alkaline earth metal ions nature on the metal binding selectivity by the *cis* **CyAla3** and **CyAla4** cyclic peptides. The second goal of this theoretical study is anticipating the efficiency of cyclic peptides for selective extracting of different metal ions. The results obtained in this work could be useful for predicting the applicability of an extractant for different metal ions, the material design of metal ion recognition and the other related fields. Also, investigation of interactions of cyclic peptides with guest molecules, as inclusion complexes, could help us to explain the features responsible for the remarkable potency of cyclic peptides.

2. Computational Methods

DFT calculations were applied to optimize the structures of selected cyclic peptides in this work. Vibrational frequency calculations were also performed to verify that the optimized structures are in local minima on their potential energy surfaces. The original geometries of cyclic peptides were taken from the structures reported by Poteau and Trinquier. [28] The optimized structures of cyclic peptides were used for studying the interaction of alkaline earth metal ions at the DFT/ B3LYP and DFT/CAM-B3LYP level of theory. Briefly, the CAM-B3LYP method combines the features of hybrid functionals such as B3LYP [61-63] with the long-range corrected functionals of Hirao et al. [61] The exchange functional is considered as a mixture of exact, i.e., Hartree–Fock and DFT exchange, but, unlike B3LYP, the ratio of exact to DFT exchange varies in different regions of the molecule. The key improvement in this method is that the short range DFT exchange interaction is incorporated in the short-range DFT exchange functional but, the correct long-range interaction is described via HF exchange. In this work a mixed basis set including 6-31+G(d) for C, H, O, N,Be^{2+}, Mg^{2+}, Ca^{2+} and the effective core potential (ECP) of LANL2DZ for Sr^{2+} and Ba^{2+} have been used for the calculations. . In addition, we decided to use B3LYP in the present study. The B3LYP functional has been widely used, and is generally considered satisfactory for alkali–ion complexes .[64-66]

All local energy minimum structures found by potential energy surface (PES) scan (relax) calculations were fully optimized at the B3LYP/6-31+G(d) level of theory. [67] For scanning metal cations, we used the following coordinate system. The proper cyclic peptide was positioned around the z-axis where all oxygen or nitrogen atoms were in the x-y plan. In addition, a dummy atom was put in the center of the macrocyle. Then, the earth alkaline metal cation was scanned along the z-axis. Initial positions were generated by movement of M^{2+} cations along the Z-axis.

Interaction energies were corrected by zero point energy (ZPE) and the basis set superposition error (BSSE) [68] was taken into account by the counterpoise method. The natural bond orbital (NBO) analysis [69,70] at the CAM-B3LYP/6-31+G(d) level of theory was performed to characterize the second-order interaction energy. All calculations were performed with the GAUSSIAN 09 computational chemistry package [71] without any limitation. The atoms in molecule (AIM) [72,74] at the CAM-B3LYP/6-31+G(d) level was used here to describe the binding characteristic between donor and acceptor.

3. Results and Discussion

3.1 Geometrical parameters: In the present study, two cyclic peptides constructed from 3 or 4 L-alanine molecules, named **CyAla3** and **CyAla4**, with amide groups in the *cis* conformation have been selected. The optimized structures for the cyclic peptides in their ground electronic states are shown in Fig. 1. Local minimum energy structures were confirmed by the absence of any imaginary frequency in the Hessian matrix. As seen in Fig. 1, the oxygen atoms in the optimized structures are pointing upward from the peptide rings. At the CAM-B3LYP level of theory, the calculated bond lengths of C=O and C-N bonds in the amide group of **CyAla3** are 1.226 and 1.369 Å, respectively. These values for the **CyAla4** ring are 1.224 and 1.359 Å, respectively. It is notable that the calculated C=O and C-N bond lengths are same in each free cyclic peptide. It is seen that the value of C-N bond length is sensitive to the ring size. In addition, with calculation at the B3LYP level, the calculated bond lengths of C=O and C-N bonds in the amide group of **CyAla3** are 1.232 and 1.375 Å, respectively. These values for the **CyAla4** ring are 1.229 and 1.365 Å, respectively. The fully relaxed minimum energy structures of the metal ion-cyclic

peptide complexes calculated at the CAM- B3LYP/6-31+G(d) and B3LYP/6-31+G(d) levels of the theory are given in Figures 2, 3 and Figure S2, S3, respectively.

CAM-B3LYP

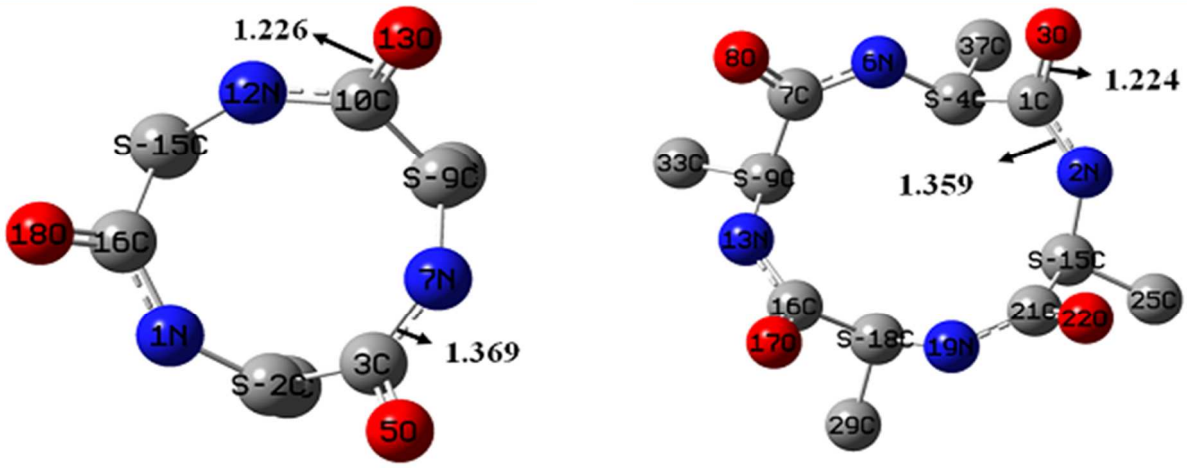

Figure.1. The optimized structures of **CyAla3** and **CyAla4** obtained at the CAM-B3LYP/6–31+G(d) level of theory (H atoms are omitted for clarity). All CO and CN bonds are identical for each free cyclic peptide.

Moreover, it is evident from figures 2, 3, S2, and S3 that the metal cations are not located in the hollow of cyclic peptides and form stable complex with three or four O atoms of the cyclic peptide backbones, where these atoms point upward to the metal ion as seen in the case of the free **CyAla3** or **CyAla4** molecules. As one can see, comparison of the calculated structural parameters of metal complexes with free cyclic petides indicates that the C=O bond lengths increase and the C(=O)-N bond lengths decrease in M^{2+}/**CyAla3**. (See figure 2.) It must be noted that in the free **CyAla3,** all carbonyl bond lengths are identical. The analysis of metal-ligand distances may be valuable. All of the alkaline earth metal cations symmetrically interact with oxygen electron lone pairs so that the calculated M-O bond lengths are 1.606, 1.994, 2.346, 2.548, 2.746 Å for the Be^{2+} , Mg^{2+}, Ca^{2+}, Sr^{2+} and Ba^{2+}, respectively. It is obvious that the M-O

bond length decreases with the decrease in the size of metal cation. The selected calculated important geometrical parameters of complexes of alkaline metal ions with **CyAla3** molecule calculated at CAM-B3LYP/6-31+G(d) levels of the theory have been tabulated in Table 1. Comparing the geometries of the free cyclic peptide **CyAla3** molecule with the corresponding cationic metal complexes indicates that the C-C(H_3) bond lengths decrease in the range of 0.020-0.008 from the Be^{2+}/**CyAla3** at top of the alkaline earth metal group to Ba^{2+}/**CyAla3** at the end of the group but the C-C(=O) bond lengths decrease from 0.004 Å for Be^{2+}/**CyAla3** and 0.001 Å for Mg^{2+}/**CyAla3**, but for Ca^{2+} to Ba^{2+} the C-C(=O) bond lengths increase about 0.001-0.002 Å. In addition, with the complex formation, the NH bond length increases in the range of 0.003-0.007 Å. For more investigation for the effect of complexation on the geometry of cyclic peptide, the dihedral angle between the carbonyl groups and N-H bonds was determined. As seen, aggregation causes non-negligible changes in the value of dihedral angles. For all Φ (H-N-C-O) dihedral angles, Be^{2+}/**CyAla3** has maximum dihedral angle and from top to end of the group dihedral angle is increase. For example, the value of Φ (H8-N7-C3-O5) dihedral angle changes from -4.4 to 24.0, 20.0, 18.6, 17.6, 16.5 degrees after complexation of **CyAla3** with metal cations including Be^{2+}, Mg^{2+}, Ca^{2+}, Sr^{2+}, and Ba^{2+} metal cations, respectively.

Table 1
The selected geometrical parameters of M/**CyAla3** complexes calculated at the CAM-B3LYP/6-31+G(d) level of theory.

M/CyAla3	C-C(=O)	C-C(H_3)	N-H	φ 8-7-3-5	φ 14-12-10-13	φ 6-1-16-18	C=O	C(=O)-N
CyAla3	1.538	1.528	1.014	-4.4	-4.5	-4.4	1.226	1.369
Be^{2+}	1.534	1.516	1.021	24.0	23.9	23.9	1.277	1.350
Mg^{2+}	1.537	1.517	1.020	20.2	20.2	20.2	1.263	1.355
Ca^{2+}	1.539	1.518	1.018	18.6	18.7	18.6	1.252	1.361
Sr^{2+}	1.539	1.519	1.017	17.6	17.6	17.5	1.248	1.364
Ba^{2+}	1.540	1.520	1.017	16.5	16.5	16.6	1.246	1.365

Bond lengths are in Å, dihedral angles in degree. Because of symmetry of free molecule and corresponding complexes only one bond length is presented in table.

The important geometrical parameters of the "host" ligand constructed from four alanine molecule (**CyAla4**) and its "host–guest" complexes with Be^{2+}, Mg^{2+}, Ca^{2+},Sr^{2+}, and Ba^{2+} ions calculated at the same level of theory than for CyAla3 are presented in table 2. It is noteworthy that in the formation of $Be^{2+}$and Mg^{2+} complexes, only two alanine carbonyl oxygen atoms interact with the metal ions as seen in figure 3. The calculated distances between two carbonyl oxygen atoms nearby $Be^{2+}$and Mg^{2+} ion in the upward cavity are 1.577 and 1.980 Å for Be^{2+}/**CyAla4** and Mg^{2+}/**CyAla4** complexes, respectively. In addition, the distance between amide nitrogens and mentioned ions are 1.917 and 2.333 Å, respectively. Figure 3 also shows that four oxygen atoms of **CyAla4** are interacting with Ca^{2+}, Sr^{2+}, and Ba^{2+} metal ions. The average bond length for the Ca–O and Sr–O bond is 2.427 Å and 2.625 Å, respectively.

Comparison of the M/**CyAla4** complexes with the corresponding free cyclic peptide molecule indicates that the C–C(=O) bond lengths in Be^{2+}/**CyAla4** and Mg^{2+}/**CyAla4** are different from the corresponding C–C(=O) bond length in free cyclic peptide (0.014-0.012 Å shift for C–C(=O) that is bound to metal ions) while for the larger metal ions the C–C(=O) bond lengths in the cationic metal complexes are almost unchanged.

Only in Be^{2+}/**CyAla4** and Mg^{2+}/**CyAla4** because of different geometry we use average values for some geometrical parameters such as C-(CH3) and N-H, but because of symmetry for other cationic metal complexes other geometrical parameters are similar. It is noted that because of the importance of C–C(=O), C=O and C(=O)-N bond lengths in Be^{2+}/**CyAla4** and Mg^{2+}/**CyAla4** we have maintained the bond lengths values for these parameters.

Table 2

The selected geometrical parameters of M/**CyAla4** complexes calculated at the CAM-B3LYP level of theory

M/CyAla4	C-C(=O)	C-(CH3)	N-H	φ 12-2-1-3	φ11-6-7-8	φ14-13-16-17	φ20-19-21-22	C=O	C(=O)-N
CyAla4	1.537 [a]	1.529 [a]	1.017 [a]	6.6	4. 3	6.6	4.3	1.224	1.359
Be^{2+}	(1.547) [b]	1.530 [a]	1.021 [a]	-15.1	119.5	-15.1	120.1	(1.191) [b]	(1.495) [b]
	1.523							1.280	1.320
Mg^{2+}	(1.549) [b]	1.527 [a]	1.024 [a]	-12.1	4.3	-12.1	4.3	(1.195) [b]	(1.475) [b]
	1.525							1.264	1.330
Ca^{2+}	1.537	1.532	1.020	-14.5	-14.5	-14.5	-14.5	1.244	1.361
Sr^{2+}	1.538	1.532	1.020	-12.9	-12.9	-12.9	-12.9	1.242	1.361
Ba^{2+}	1.538	1.532	1.019	-11.5	-11.5	-11.5	-11.5	1.240	1.361

Bond lengths in Å, dihedral angles in degree, [a] the average value, [b] the values in parenthesis are the distance between metal ions and faraway atoms.

Similar results have been obtained with B3LYP. The selected important calculated geometrical parameters of complexes of alkaline metal ions with **CyAla3** molecule calculated at B3LYP/6-31+G(d) levels of the theory have been tabulated in Table S.1 and structures are shown in figure S.2.

All of the alkaline earth metals cations are approximately symmetrically interact with oxygen lone electron pairs so that the calculated M-O bond lengths are 1.612, 2.008, 2.363, 2.567, 2.768 Å for the Be^{2+} , Mg^{2+}, Ca^{2+}, Sr^{2+} and Ba^{2+}, respectively. The results of geometrical parameters of the metal complexes of $[M/CyAla4]^{2+}$ that are similar to result of calculation with CAM- B3LYP method are presented in Figure S.3. In the formation of $Be^{2+}$and Mg^{2+} complexes, only two alanine carbonyl oxygen atoms interact with the metal ions. The calculated distances between two carbonyl oxygen atoms nearby $Be^{2+}$and Mg^{2+} ion in the upward cavity are 1.585 and 1.993 Å for the Be^{2+}/**CyAla4** and Mg^{2+}/**CyAla4** complexes, respectively. In addition, the distance between amide nitrogens and mentioned ions are 1.931, 1.937 and 2.360, 2.358 Å, respectively. Figure S.3 also shows that four oxygen atoms of **CyAla4** are interacting with Ca^{2+}, Sr^{2+}, and Ba^{2+} metal ions. The bond length for the Ca–O, Sr–O and Ba-O bond is 2.451 Å , 2.653 Å and 2.846 Å respectively.

Comparison of M/**CyAla4** complexes with the corresponding free cyclic peptide molecule indicates that the C–C(=O) bond lengths in Be^{2+}/**CyAla4** and Mg^{2+}/**CyAla4** are different from the corresponding C–C(=O) bond in free cyclic peptide(0.026-0.015 Å for C–C(=O) that is bond to metal ions) while for larger metal ions the C–C(=O) bond lengths in the cationic metal complexes are almost unchanged. The rest of important geometrical parameters listed in Table S.1.

13

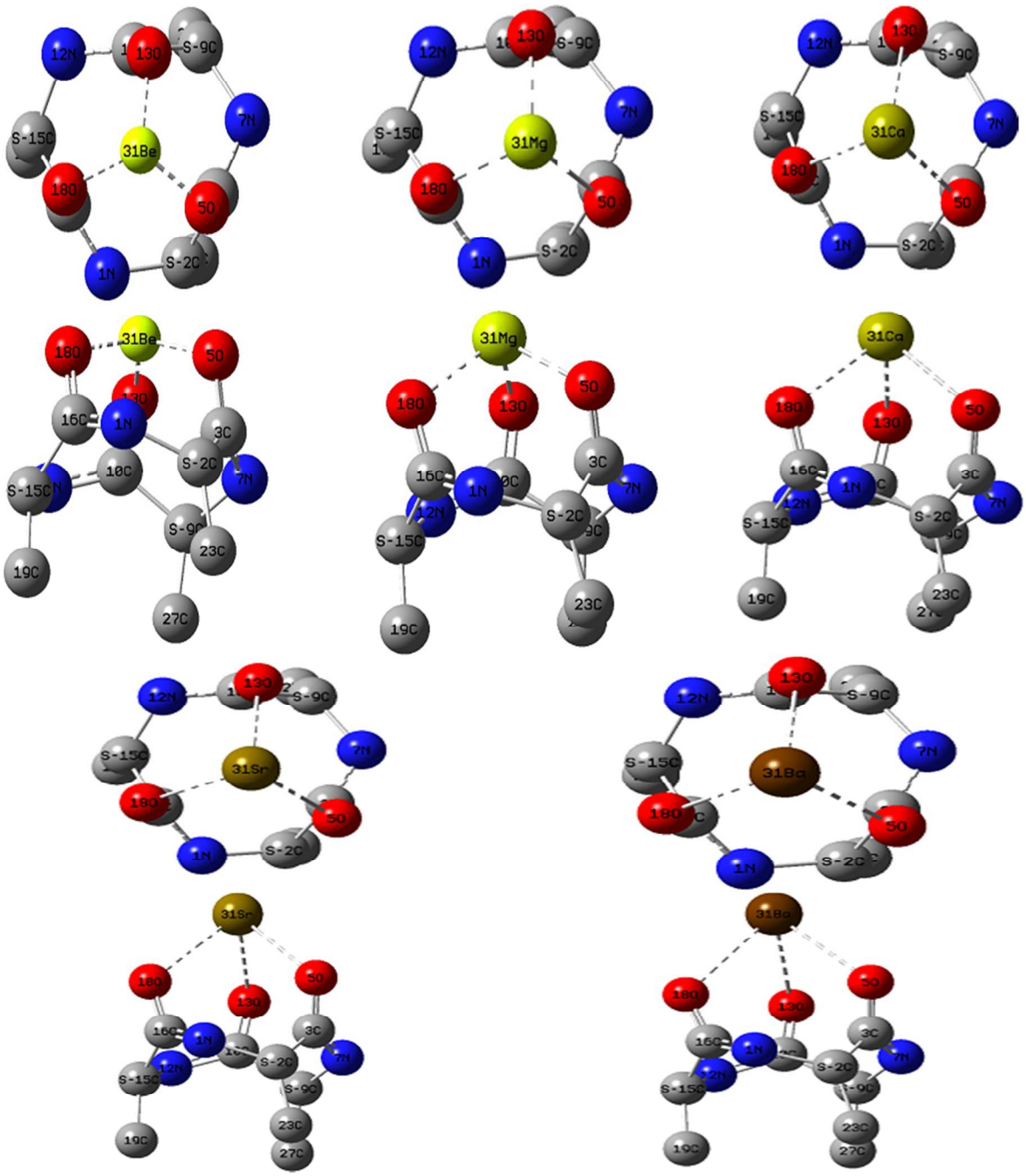

1

2 **Figure.2.** Optimized structures and important geometrical parameters of M/**CyAla3** complexes calculated at the

3 CAM-B3LYP level of theory, M= Be^{2+}, Mg^{2+}, Ca^{2+}, Sr^{2+} and Ba^{2+}

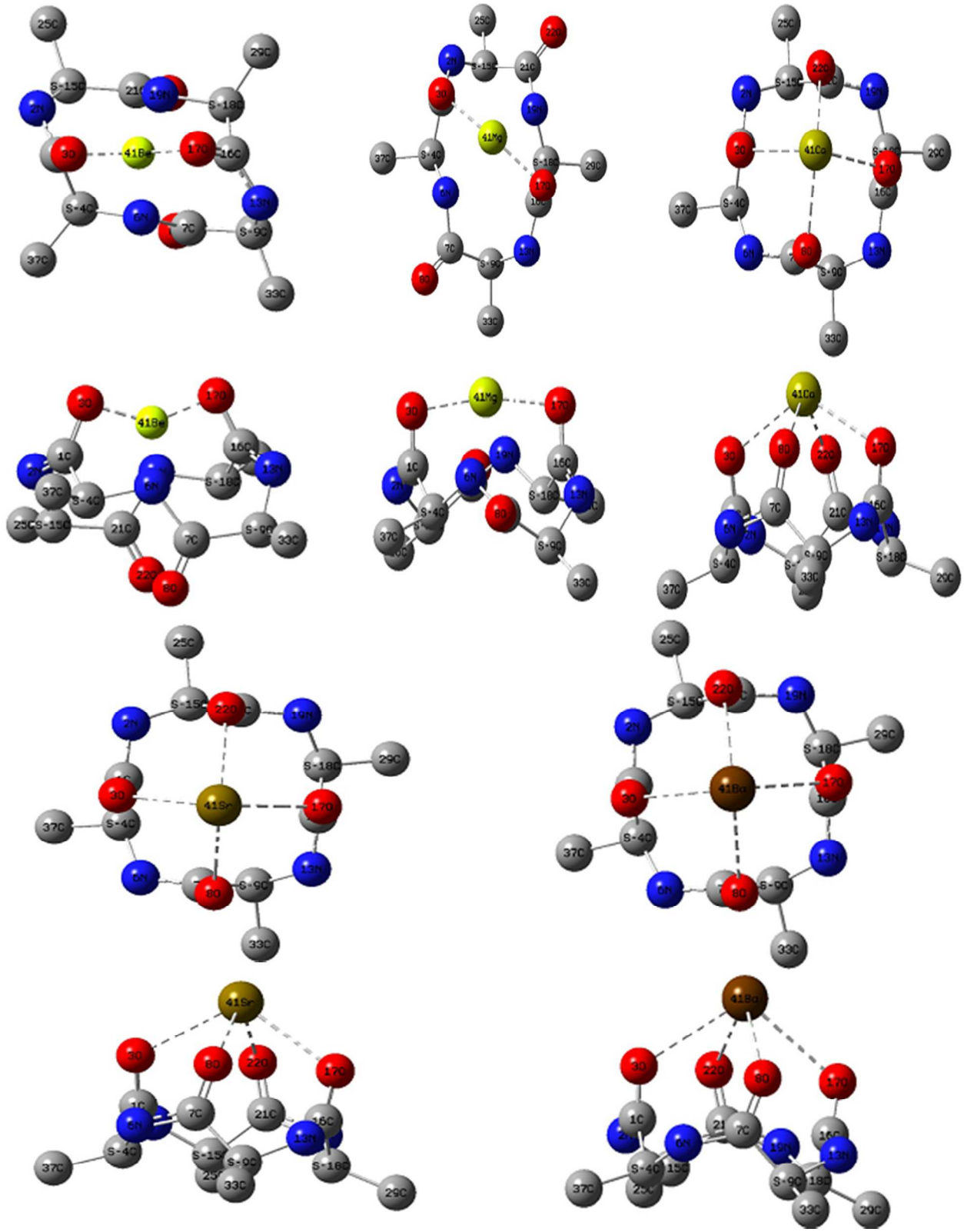

Figure.3. Optimized structures and important geometrical parameters of M/**CyAla4** complexes calculated at the CAM-B3LYP level of theory, M= Be^{2+}, Mg^{2+}, Ca^{2+},Sr^{2+} and Ba^{2+}

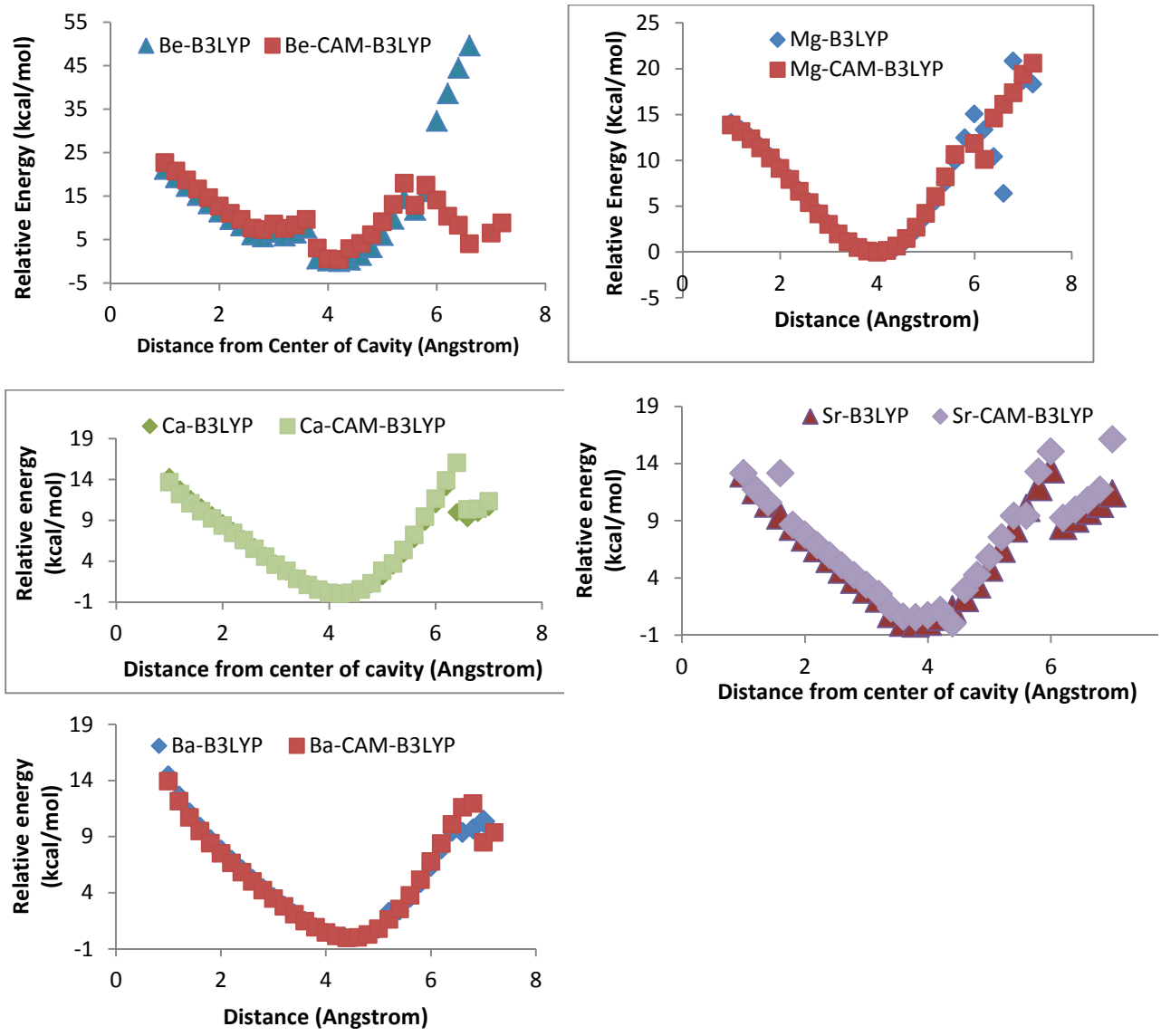

Figure.4. Potential energy surfaces of inclusion complexation of metal cations in the cavity of **CyAla3** at different positions, calculated at B3LYP/6-31+G(d) and CAM-B3LYP levels of theory

For more precise evaluation of the correct position of metal cations in the cavity of cyclic peptides, an exploration of the PES has been performed. For this purpose, the position of relevant metal cations was changed from the cavity center of cyclic peptide by 0.2 Å intervals. The graphical illustration of the energy changes occurring during the inclusion passing process of

cations at different Z positions of cyclic peptides presented in Figure 4. A closer look at this figure and comparison with geometrical parameters allows one remarking that inclusion process is thermodynamically favorable. Interestingly, a local minimum found for each cation about 6.4 Å above the cavity center. It is interesting that for the Be cation, a considerable local minimum related to method of calculation (CAM-B3LYP level) at 6.2 Å, found.

3.2. Binding energies and metal binding selectivity

Generally, the energy decreases with creation of a host–guest complex. The decreased energy is called the binding energy (BE), which is associated with the solidity of the equivalent host–guest complex and the extraction power of an extractant for a given metal ion. A steady complex all the time gives a negative value of ΔE. Therefore, the stability of complexes will increase with the negative value of ΔE, and the extraction power of an extractant for metal ions will be stronger. The BE of M/**CyAla3** or M/**CyAla4** complexes for the complexation reaction:

$$M^{2+} + CyAla3 \longrightarrow M/CyAla3 \quad (1)$$

is defined by the following general equation:

$$BE = E_{M^{2+}/CyAla} - (E_{M^{2+}} + E_{CyAla}) \quad (2)$$

where $E_{M^{2+}/CyAla}$, $E_{M^{2+}}$, and E_{CyAla} refer to the energy of the M^{2+}/**CyAla** complex, M^{2+} ion and the cyclic peptide system, respectively. The calculated binding energies using B3LYP and CAM-B3LYP methods are listed in Table 3. The results clearly show the effect of the metal ion's nature on the selective binding capacity.

The order of binding energies are Be^{2+} > Mg^{2+}> Ca^{2+} > Sr^{2+} > Ba^{2+} for both M/**CyAla3** and M/**CyAla4.** The binding energies were also corrected for ZPE and BSSE corrections (ΔE_{ZPE} and ΔEcorr in Table 3). The binding enthalpy (ΔH) and binding free energy (ΔG) for the metal cyclic peptide complexation reactions were also calculated at the CAM-B3LYP and B3LYP levels at 298 K and the results have been listed in Table 3. It is obvious that the formation of metal ion complexes is exothermic as revealed from the values of ΔH given in Table 3. The binding enthalpy is increased in the order of Be^{2+} > Mg^{2+} > Ca^{2+} > Sr^{2+} > Ba^{2+} for both B3LYP and CAM- B3LYP methods. It is notable that with respect to the same cation, the larger cavity **CyAla4** ligand, can hold the alkaline metal cations better than **CyAla3** molecule**.** One can evaluate the regularity of B3LYP and CAM-B3LYP methods with looking to figure. 5 which demonstrates a good correlation between the two levels of theory.

Table 3

The binding energies ΔE (kcal/mol), zero point corrected binding energies ΔE_{ZPE} = (ΔE+ΔZPE), the value of basis set superposition error in energy (E_{BSSE}), ΔEcorr= ΔE_{ZPE}+ E_{BSSE}, binding enthalpies, Gibbs free energies ΔG of binding (kcal/mol) and formation equilibrium constants in gas phase for the complexes calculated at B3LYP and CAM-B3LYP levels of theory.

CAM-B3LYP	ΔE	ΔE_{ZPE}	E_{BSSE}	ΔEcorr	ΔH	ΔG	Log K
M/CyAla3							
Be^{2+}	-327.09	-324.14	1.25	-322.89	-326.47	-311.86	228.64
Mg^{2+}	-205.23	-203.37	1.34	-202.03	-205.07	-190.98	140.01
Ca^{2+}	-139.85	-138.38	1.20	-137.18	-139.71	-126.25	92.56
Sr^{2+}	-106.58	-105.39	1.47	-103.92	-106.44	-93.46	68.52
Ba^{2+}	-90.17	-89.10	1.38	-87.72	-90.01	-77.40	56.74
M/CyAla4							
Be^{2+}	-359.83	-356.61	1.78	-354.83	-358.64	-345.92	253.60
Mg^{2+}	-207.52	-205.61	1.99	-203.62	-206.97	-195.07	143.01
Ca^{2+}	-151.59	-149.89	1.40	-148.49	-151.18	-138.33	101.42
Sr^{2+}	-116.42	-114.97	1.77	113.20	-115.98	-103.61	75.96
Ba^{2+}	-99.49	-98.23	1.75	-96.48	-99.06	-87.17	63.91
B3LYP							
M/CyAla3							
Be^{2+}	-322.65	-319.82	1.19	-318.63	-321.51	-309.53	226.93
Mg^{2+}	-200.63	-198.82	1.26	-197.56	-199.91	-188.40	138.12

18

Ca^{2+}	-135.48	-134.01	1.17	-132.84	-134.72	-123.89	90.83
Sr^{2+}	-102.51	-101.24	1.42	-99.82	-101.70	-91.28	66.92
Ba^{2+}	-86.29	-85.19	1.36	-83.83	-85.47	-75.53	55.37
M/CyAla4							
Be^{2+}	-354.26	-351.17	1.79	-349.38	-353.13	-340.49	249.62
Mg^{2+}	-203.24	-201.51	1.88	-199.63	-202.80	-191.00	140.03
Ca^{2+}	-146.32	-144.73	1.28	-143.45	-145.97	-133.18	97.64
Sr^{2+}	-111.59	-110.18	1.69	-108.49	-111.11	-98.96	72.55
Ba^{2+}	-95.03	-93.77	1.74	-92.03	-94.59	-82.74	60.66

ΔE and ΔG in kcal/mol

The calculated binding energies for the earth alkaline metal cations are much higher than with our previously reported data for the complexation of alkali metal cations and above mentioned cyclic peptides. [44] The range of binding energies for the alkali metal cations has been found to be 47.11-15.75 and 31.19-15.24 kcal/mol for the M/**CyAla3** and M/**CyAla4**, respectively. As it can be seen, alkaline earth metal cations form more tighten complexes with cyclic peptides.

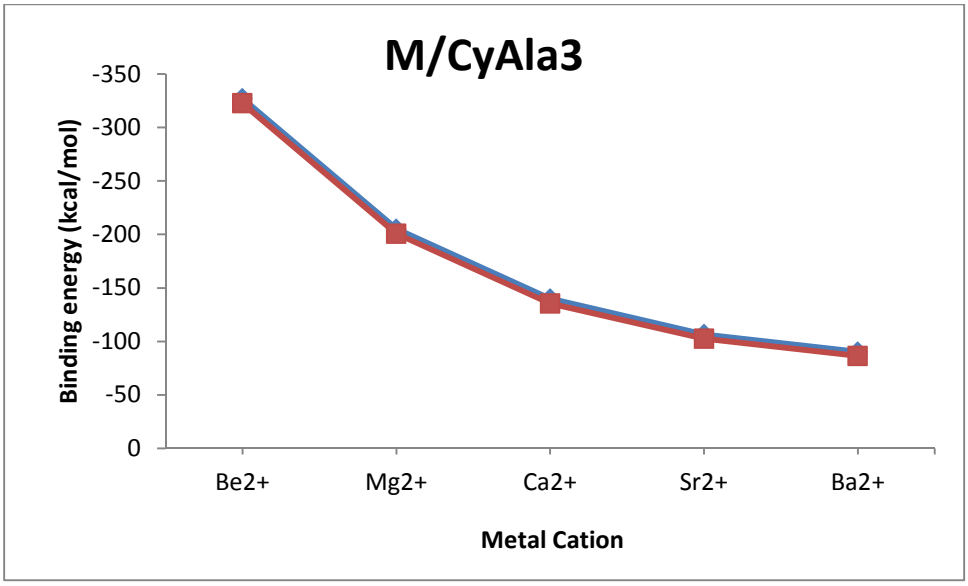

19

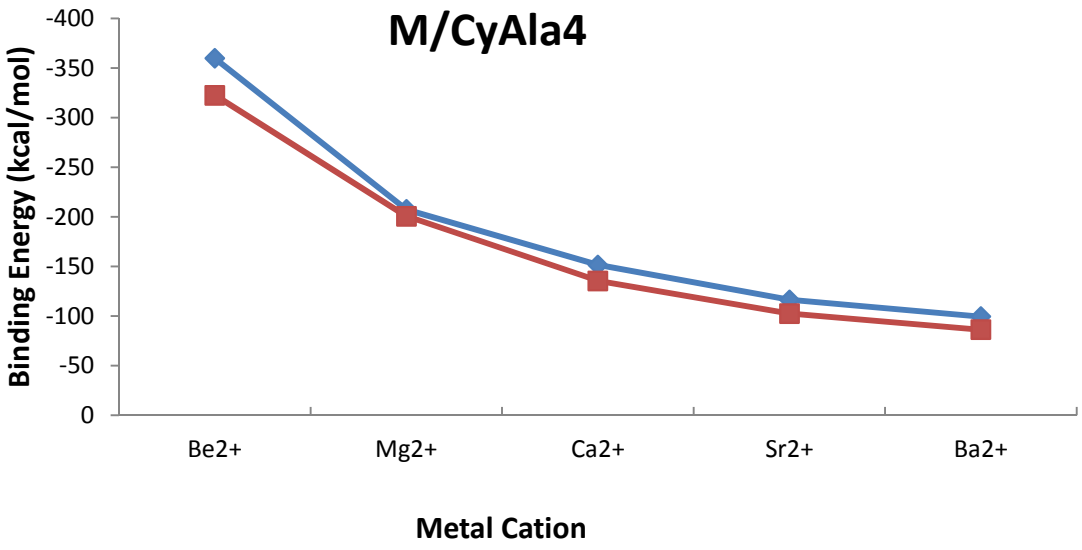

Figure.5. Correlation between B3LYP (red curve) and CAM-B3LYP (blue curve) binding energies for M/**CyAla3** and M/**CyAla4** complexes.

3.3. Second-order interaction energies, energy gaps and charge transfers

To find the origin of the favorable interaction energies and clarify the reason for the different metal binding selectivity, the NBO analysis was carried out in this work. In NBO analysis, the stabilization energy ($E^{(2)}$) is related to the strength of the coordination interaction. There is a direct relationship between the stability of complex and ($E^{(2)}$) so that the more stability of complex is corresponds to the larger value for $E^{(2)}$. The stabilization energy $E^{(2)}$, associated with i→j delocalization, can be estimated by the following equation:

$$E^{(2)} = \Delta E_{ij} = q_i \times \frac{F^2(i,j)}{\varepsilon_i - \varepsilon_j}$$

where q_i is the donor orbital occupancy, ε_i and ε_j are orbital energies of donor and acceptor orbitals, respectively. F(i,j) are off-diagonal elements associated with NBO Fock matrix. The values of $E^{(2)}$, obtained by NBO analysis, for the considered complexes are summarized in Table 4. The value of stabilization energy depends on the strength of the charge-transfer interaction between a Lewis type NBOs (donor) and non-Lewis NBOs (acceptor). The stronger donor→acceptor interaction leads to the higher value for the relevant stabilization energy, and more charge will be transferred from the donor (cyclic peptide) to the acceptor (metal ion). Overall, the results of NBO analysis indicate that the origin of the interactions between the metal cations and the electron-donating oxygen or nitrogen atoms in the considered cyclic peptides are electrostatic. It is notable that for the M/**CyAla3** complexes, with going from Be^{2+} as the smallest cation to Ba^{2+} as the largest one, the electron donation of oxygen atoms decreases from 17.24 to 1.38 kcal/mol, respectively. However for the M/**CyAla4** complexes when Mg^{2+} located in the cavity of ligand, the lone electron pairs of both N and O atoms contribute in stabilizing the cation. In addition, the values of $E^{(2)}$ for the M/**CyAla3** complexes are lower than those for the M/**CyAla4** when the same alkali metal cation contribute in the complexation.

Table 4
Selected stabilization interaction $E^{(2)}$ (kcal/mol)for M/**CyAla3**and M/**CyAla4** complexes at the CAM-B3LYP level of theory.

M/**CyAla3**			M/**CyAla4**		
Donor	Acceptor		Donor	Acceptor	
Be^{2+}			Be^{2+}		
BD(1)C3-O5	LP*(1)Be31	4.99	BD(1)O3-Be41	BD*(2)C1-N2	88.55
BD(2)C3-O5	LP*(1)Be31	10.71	BD(1)O17-Be41	BD*(2)N13-C16	88.41
BD(2)C3-O5	RY*(1)Be31	3.55	LP(1)O3	BD*(1)O3-Be41	8.09
BD(1)C10-O13	LP*(1)Be31	4.87	LP (1)O3	BD*(1)O17-Be41	6.44
BD(1) C16-O18	LP*(1)Be31	4.99	LP(2)O3	BD*(1)O3-Be41	6.81
BD(2)C16-O18	LP*(1)Be31	10.69	LP(1)N6	BD*(1)O17-Be41	6.83
BD(2)C16-O18	RY*(2)Be31	4.33	LP(1)O17	BD*(1)O3-Be41	6.45
LP(1)O5	LP*(1)Be31	17.24	LP(1)O17	BD*(1)O17-Be41	8.20
LP(2)O5	LP*(1)Be31	22.63	LP(2)O17	BD*(1)O17-Be41	6.61

LP(1)O13	LP*(1)Be31	17.12	LP(1)N19	BD*(1)O3-Be41	6.77
LP(2)O13	LP*(1)Be31	22.42	LP(1)N19	BD*(1)O17-Be41	5.28
LP(3)O13	LP*(1)Be31	14.90			
LP(1)O18	LP*(1)Be31	17.24			
LP(2)O18	LP*(1)Be31	22.63			
Mg^{2+}			Mg^{2+}		
LP(2)O5	LP*(1)Mg31	4.67	BD(2)C1-O3	LP*(1)Mg41	8.28
LP(1)O13	LP*(1)Mg31	10.23	LP(1)O3	LP*(1)Mg41	11.73
LP(2)O13	LP*(1)Mg31	4.64	LP(1)N6	LP*(1)Mg41	14.99
LP(1)O18	LP*(1)Mg31	10.22	LP(1)O17	LP*(1)Mg41	11.64
LP(2)O18	LP*(1)Mg31	4.66	LP(3)O17	LP*(1)Mg41	10.29
			LP(1)N19	LP*(1)Mg41	15.01
Ca^{2+}			Ca^{2+}		
LP(1)O5	LP*(1)Ca31	4.22	LP(1)O3	LP*(1)Ca41	4.94
LP(1)O13	LP*(1)Ca31	4.21	LP(1)O8	LP*(1)Ca41	4.93
LP(1)O18	LP*(1)Ca31	4.21	LP(1)O17	LP*(1)Ca41	4.94
			LP(1)O22	LP*(1)Ca41	4.94
Sr^{2+}			Sr^{2+}		
LP(1)O5	LP*(1)Sr31	2.90	LP(1)O3	LP*(3)Sr41	7.78
LP(2)O5	RY*(2)Sr31	1.02	LP (1)O8	LP*(1)Sr41	5.33
LP(1)O13	LP*(1)Sr31	2.92	LP (1)O8	LP*(2)Sr41	7.78
LP(1)O18	LP*(1)Sr31	2.92	LP(1)O17	LP*(1)Sr41	5.34
LP(2)O18	RY*(1)Sr31	1.05	LP(1)O17	LP*(3)Sr41	7.78
			LP(1)O22	LP*(1)Sr41	5.34
			LP(1)O22	LP*(2)Sr41	7.78
Ba^{2+}			Ba^{2+}		
LP(1)O5	LP*(1)Ba31	1.38	LP(1)O3	LP*(1)Ba41	1.81
LP(1)O13	LP*(1)Ba31	1.38	LP(1)O8	LP*(1)Ba41	1.81
LP(2)O13	RY*(2)Ba31	1.00	LP(1)O17	LP*(1)Ba41	1.81
LP(1)O18	LP*(1)Ba31	1.39	LP(1)O22	LP*(1)Ba41	1.81

LP, 1-center valence lone pair (LP1 and LP2 are the tow lone pairs of each oxygen and nitrogen atoms, respectively. One of the NBO is in the plane, the other is the corresponding NBO perpendicular to the plane): LP*, 1-center valance antibond lone pair: BD, 2-center bond. RY* corresponds to Rydberg NBOs.

In order to analyze the electrostatic interactions of the alkaline metal cations with the host molecules, the partial charges of the selected atoms in the complexes compared with the corresponding charges in the free ligand molecules, (See Table 5). It is well known that the complexation of metal ions and peptides can proceed through the electrostatic effects taking place between metal ions with main chain carbonyl groups or side chains groups. However, molecular modeling and experimental results suggested the preference of the interaction of backbone carbonyl groups of cyclic peptides with the metal ions inside the cavity. [75,77] For the

present complexes, the charge–transfer is defined as the charge difference between a free metal ion and its complexated form.

Table 5
Calculated NBO charges of the metals and selected atoms of M/**CyAla3** and M/**CyAla4 complexes** at CAM-B3LYP level of theory

CyAla3		Be^{2+}	Mg^{2+}	Ca^{2+}	Sr^{2+}	Ba^{2+}
N1	-0.671	-0.609	-0.619	-0.632	-0.636	-0.640
N7	-0.671	-0.609	-0.619	-0.632	-0.637	-0.639
N12	-0.671	-0.609	-0.619	-0.632	-0.637	-0.640
O5	-0.627	-0.837	-0.809	-0.787	-0.770	-0.759
O13	-0.627	-0.837	-0.809	-0.786	-0.770	-0.758
O18	-0.627	-0.837	-0.809	-0.787	-0.771	-0.759
M		1.744	1.856	1.942	1.918	1.931
CyAla4						
N2	-0.651	-0.579	-0.597	-0.646	-0.645	-0.649
N6	-0.654	-0.914	-0.871	-0.646	-0.645	-0.649
N13	-0.651	-0.579	-0.597	-0.646	-0.645	-0.649
N19	-0.654	-0.913	-0.871	-0.646	-0.645	-0.649
O3	-0.635	-0.831	-0.793	-0.752	-0.716	-0.736
O8	-0.635	-0.461	-0.453	-0.751	-0.716	-0.736
O17	-0.635	-0.831	-0.793	-0.752	-0.716	-0.736
O22	-0.635	-0.461	-0.453	-0.752	-0.716	-0.736
M		1.697	1.805	1.932	1.763	1.932

Table 5 also reveals that for the M/**CyAla3**, the negative charge on the nitrogen atoms changed from -0.671 esu in the free **CyAla3** molecule to -0.609, -0.619, -0.632, -0.636, and -0.640 esu for the Be^{2+}, Mg^{2+}, Ca^{2+}, Sr^{2+} and Ba^{2+} metal cations, respectively. Moreover, the negative charge on the oxygen atoms increases from -0.627 esu in the free cyclic peptide molecule to -0.837, -0.809, -0.787, -0.770, and -0.759 esu for the Be^{2+}, Mg^{2+}, Ca^{2+}, Sr^{2+} and Ba^{2+} metal cations located in the cavity of cyclic peptide, respectively. The charge transfer values for the metal ions in the complex are 0.256, 0.144, 0.038, 0.082 and 0.069 esu, calculated for the Be^{2+}, Mg^{2+}, Ca^{2+}, Sr^{2+} and Ba^{2+} metal cations, respectively. For the Be^{2+} cation that interacts with contrary nitrogen atoms, N2 and N13 atoms take -0.651 but N6 and N19 atoms take -0.654 esu for the Be^{2+}/**CyAla4,** respectively**.** In addition, for the Mg^{2+}/**CyAla4** complex the N2 and N13 atoms

take -0.579 esu but, N6 and N19 atoms take -0.914 esu, respectively. As you can see the charge transfer values are in accordance with the radii of metal cations.

3.6. AIM topological parameters

The theory of atoms in molecules (AIM) was developed by Professor Richard F. W. Bader and his coworkers, in 1990. [72,73] AIM characterizes the chemical bonding of a system based on the topology of the quantum charge density. The bond critical point (BCP) is described in terms of topological parameters, such as the charge density and the corresponding Laplacian field. According to the topological analysis of electronic charge density in AIM theory, electronic charge density $\rho(r)$ describes the strength of a bond (If $\rho(r)$ value is big, the corresponding bond will be strong), and Laplacian of the electron charge density $\nabla^2\rho(r)$ (The sum of eigenvalues ($\lambda1$,$\lambda2$ and $\lambda3$) of the Hessian matrix of electronic charge density is equal to the Laplacian) shows the characteristic of the bond. A negative value of Laplacian $\nabla^2\rho(r) <0$ indicates the concentration of the electron density in the interatomic region and occurs for sharing interactions like covalent bonds whereas a positive value ($\nabla^2\rho(r) >0$) of Laplacian indicates the depletion of the electron density for the interaction of the closed-shell systems such as ionic bond, coordination bond, hydrogen bond, or van der Waals interaction. The values of $\rho(r)$, $\nabla^2\rho(r)$, the eigenvalues of the Hessian matrix and the ellipticity at the bond critical point of all studied complexes, calculated using the wave function obtained at the CAM-B3LYP/6-31+G(d) level of theory were listed in Table 6. As an example the molecular graphs of the Ca^{2+}/ **CyAla3** and Ca^{2+}/ **CyAla4** based on AIM theory are shown in Figure 6, because the other M^{2+}/ **CyAla3** and M^{2+}/ **CyAla4** have similar shape we just show one graph. Based on Table 6, the calculated Laplacian values at corresponding BCP are positive and this means that interactions between cyclic peptide

and alkaline earth metal cations were closed-shell interactions and there is no bond between them. On the other hand, the values of $\nabla^2\rho(r)$ changed in the order of $Be^{2+} > Mg^{2+} > Ca^{2+} > Sr^{2+} > Ba^{2+}$ for both M/**CyAla3** and M/**CyAla4** complexes. For all complexes except for Be/**CyAla4** and Mg/**CyAla4,** the alkaline earth metal cations interact with O atoms of cyclic peptides and as it is obvious from fig.3 the shape of these complexes are symmetrical so the interactions between alkaline earth metal cations and all of the O atoms in one complex are nearly the same. The $\rho(r)$ values show that when we go from top to end of the alkaline earth metal group, electronic charge density decreases so the interactions between cyclic peptide and alkaline earth metal cations weakens.

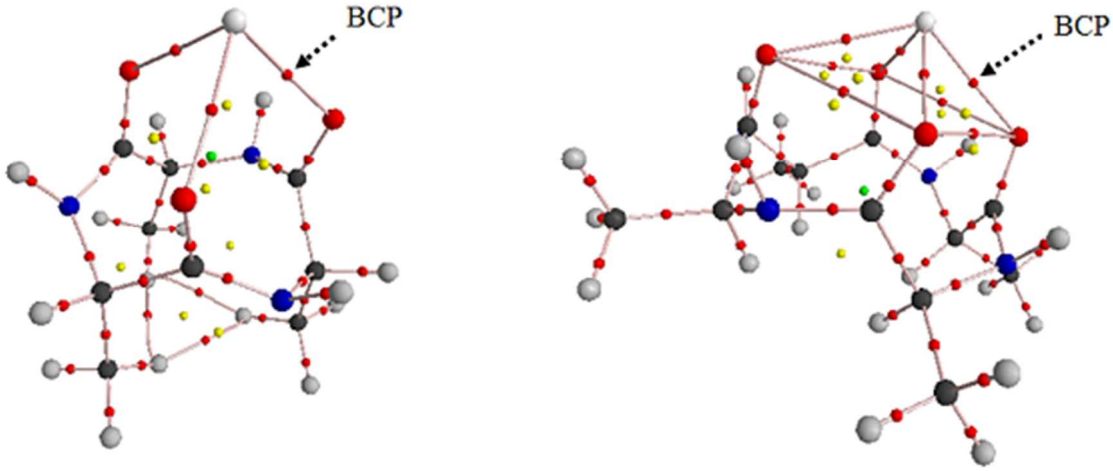

Figure.6. Molecular graphs of the Ca^{2+}/**CyAla3** and Ca^{2+}/**CyAla4** complexes at the CAM-B3LYP/6-31+G(d) level of theory.

Table 6
The topological properties at BCP of complexes

CyAla3	BCPs	λ1	λ2	λ3	$\rho_{(r)}$	$\nabla^2\rho(r)$
Be	O5 - M	-0.1755	-0.1630	0.8959	0.0787	0.5574
	O13 - M	-0.1754	-0.1629	0.8952	0.0786	0.5569
	O18 - M	-0.1755	-0.1630	0.8961	0.0787	0.5575
Mg	O5 - M	-0.0642	-0.0605	0.4511	0.0432	0.3264
	O13 - M	-0.0642	-0.0605	0.4510	0.0431	0.3264
	O18 - M	-0.0641	-0.0605	0.4509	0.0431	0.3262
Ca	O5 - M	-0.0406	-0.0376	0.2676	0.0341	0.1894
	O13 - M	-0.0405	-0.0375	0.2668	0.0341	0.1888
	O18 - M	-0.0405	-0.0375	0.2669	0.0341	0.1889

Sr	O5 - M	-0.0259	-0.0255	0.1914	0.0245	0.1400
	O13 - M	-0.0261	-0.0256	0.1925	0.0246	0.1409
	O18 - M	-0.0262	-0.0257	0.1932	0.0247	0.1414
Ba	O5 - M	-0.0225	-0.0207	0.1652	0.0230	0.1219
	O13 - M	-0.0224	-0.0206	0.1641	0.0229	0.1212
	O18 - M	-0.0225	-0.0208	0.1653	0.0231	0.1221
CyAla4						
Be	O3 - M	-0.2015	-0.1923	1.0215	0.0872	0.6277
	O17 - M	-0.2016	-0.1924	1.0221	0.0873	0.6281
	N6 - M	-0.0676	-0.0520	0.3339	0.0461	0.2143
	N19 - M	-0.0657	-0.0501	0.3259	0.0455	0.2101
Mg	O3 - M	-0.0688	-0.0653	0.4835	0.0463	0.3494
	O17 - M	-0.0689	-0.0653	0.4838	0.0463	0.3496
	N6 - M	-0.0292	-0.0244	0.1787	0.0261	0.1251
	N19 - M	-0.0293	-0.0245	0.1793	0.0261	0.1255
Ca	O3 - M	-0.0314	-0.0293	0.2076	0.0280	0.1469
	O8 - M	-0.0313	-0.0293	0.2072	0.0280	0.1466
	O17 - M	-0.0313	-0.0293	0.2075	0.0280	0.1468
	O22 - M	-0.0314	-0.0293	0.2076	0.0280	0.1469
Sr	O3 - M	-0.0206	-0.0204	0.1508	0.0205	0.1098
	O8 - M	-0.0206	-0.0204	0.1507	0.0205	0.1097
	O17 - M	-0.0206	-0.0204	0.1508	0.0205	0.1098
	O22 - M	-0.0206	-0.0204	0.1507	0.0205	0.1098
Ba	O3 - M	-0.0183	-0.0169	0.1358	0.0196	0.1005
	O8 - M	-0.0183	-0.0169	0.1357	0.0195	0.1005
	O17 - M	-0.0182	-0.0169	0.1356	0.0195	0.1004
	O22 - M	-0.0183	-0.0169	0.1357	0.0195	0.1004

($\rho_{(r)}$ in e/a_u3, $\nabla^2\rho$(r) in e/a_u5).

3.7. The HOMO and LUMO energies and the values of the energy gap

In this part we examine the highest occupied molecular orbital (HOMO) and lowest unoccupied molecular orbital (LUMO) of our complexes. HOMO and LUMO of molecules are quite essential to describe their reactivity. E_{HOMO} depicts the molecular ability in donating electrons to appropriate acceptor molecules with low energy having empty molecular orbital. In contrast E_{LUMO} indicates the ability of the molecule to accept electrons. The lower value of E_{LUMO}, indicates that the molecule would accept electrons. Therefore, relating to the value of the energy gap, $\Delta E(E_{LUMO}–E_{HOMO})$, if this energy is high it means that the reactivity to a molecule is low on the contrary if the energy gap is low the reactivity to a molecule is high because the energy

needed to promote one electron from the HOMO to the LOMO orbital will be low. The diagrams of frontier molecular orbital and the energies of Be^{2+}, Mg^{2+}, Ca^{2+}, Sr^{2+} and Ba^{2+} complexes with **CyAla3** and **CyAla4** such as E_{LUMO}, E_{HOMO}, and ΔE (in eV) estimated by the CAM-B3LYP/6-31+G(d) level are represented in Table 7 and figure 7. As one can see, for the **CyAla3** and **CyAla4** complexes, the HOMOs locate on heteroatoms of cyclic peptides. On the other hand the LUMOs show different patterns. For instance for the Be/**CyAla3** or Be/**CyAla4** complexes the LUMOs locate partly on the cation, for the other complexes the LUMOs extend on the whole molecule.

Table 7
Frontier molecular orbital diagrams and energies(eV) of Be^{2+}, Mg^{2+}, Ca^{2+}, Sr^{2+} and Ba^{2+} complexes with **CyAla3** and **CyAla4** estimated by the CAM- B3LYP/6-31+G(d) level.

M/**CyAla3**	E_{HOMO}	E_{LUMO}	ΔE	M/**CyAla4**	E_{HOMO}	E_{LUMO}	ΔE
Be	-0.669	-0.428	0.241	Be	-0.610	-0.503	0.107
Mg	-0.666	-0.386	0.280	Mg	-0.596	-0.483	0.113
Ca	-0.661	-0.357	0.304	Ca	-0.587	-0.386	0.201
Sr	-0.605	-0.312	0.293	Sr	-0.573	-0.360	0.213
Ba	-0.607	-0.309	0.298	Ba	-0.579	-0.307	0.272

As seen in Table 7 the values of E_{HOMO} for M/**CyAla3** complexes show the ranking Be^{2+}> Mg^{2+}> Ca^{2+}> Ba^{2+} > Sr^{2+} for this property. In addition, the values of ΔE show Ca^{2+}> Ba^{2+} >Sr^{2+} > Mg^{2+}> Be^{2+}. For M/**CyAla4** complexes the order is Be^{2+}> Mg^{2+}> Ca^{2+}> Ba^{2+} >Sr^{2+} for the E_{HOMO} and the values of ΔE show Ba^{2+} >Sr^{2+} > Ca^{2+} > Mg^{2+} > Be^{2+}. As can be seen from the HOMO and LUMO pictures in figure 7, the majority of HOMO and LUMO's are found on the donor atoms in the cyclic peptide.

27

HOMO	LUMO	HOMO	LUMO
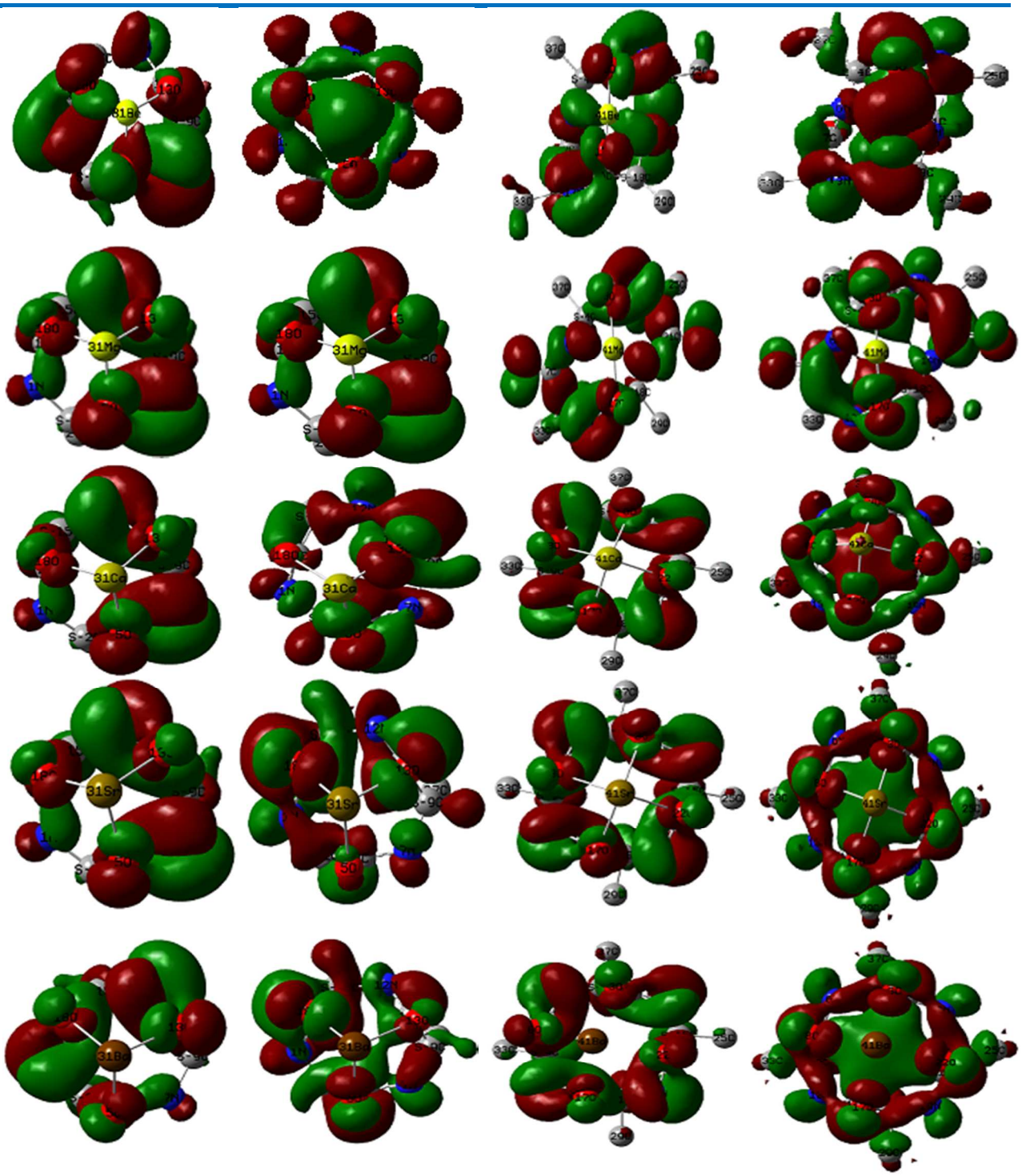			

Figure.7. Frontier molecular orbital diagrams of Be^{2+}, Mg^{2+}, Ca^{2+}, Sr^{2+} and Ba^{2+} from top to bottom complexes with **CyAla3**(left) and **CyAla4** (right) calculated at the CAM- B3LYP/6-31+G(d) level.

4. Conclusion

The structure and interaction energies of nanotubular cyclic peptide complexes of M^{2+}/**CyAla3** and M^{2+}/**CyAla4,** where M = Be^{2+}, Mg^{2+}, Ca^{2+}, Sr^{2+}, and Ba^{2+} have been studied using B3LYP and CAM-B3LYP method. The key findings are as follows:

1. Analyzing the geometry of M/**CyAla3** and M/C**yAla4** complexes indicated that the aggregation caused substantial changes in geometrical parameters of ligands. In this manner, after insertion the metal ions in the cavity of cyclic peptides, the C=O bond length increases in the range of 0.026-0.051 Å for the M/**CyAla3** complexes while the C-N amide bond length decreased in the range of 0.004-0.019 Å. In addition, for the M/**CyAla4** complexes, during the formation of $Be^{2+}$and Mg^{2+} complexes, only two alanine carbonyl oxygen atoms interact with the metal ions. Moreover, the calculated metal ligand bond lengths decrease with decreasing size of metal cation.
2. Vibrational frequency calculations showed that these cyclic peptides and their complexes with the alkaline earth metal cations are all located at local minimum points of their potential energy surfaces. Therefore, they are all stable ‘‘host–guest’’ complexes.
3. The order of binding energies calculated by B3LYP and CAM- B3LYP methods was found to be $Be^{2+} > Mg^{2+} > Ca^{2+} > Sr^{2+} > Ba^{2+}$ for both M/**CyAla3** and M/**CyAla4**, respectively. This trend indicates that these cyclic peptides might be used for separating agent of these cations.

4. Based on the charges obtained by the NBO analysis, it can be concluded that the binding energies may be attributed to the strong polarization of the C=O bonds of cyclic peptides by metal cations.
5. Based on AIM calculations, Laplacian values at corresponding BCP are positive and this means that the interactions between cyclic peptide and alkaline earth metal cations are closed-shell interactions and there is no bond between them.
6. The results of this study are comparable with our previous work. The results indicate that alkaline earth metal cations bind with much more strength than alkali metal cations. This could be due to the double positive charge of the former ions, compared to the single charge of alkali metal cations.

Acknowledge

We would like to thank Isfahan University of Technology (IUT) for the financial support (Research Council Grant).

References

1. J.M. Lehn, *Pure. Appl. Chem.* 1978, **50**, 871–892
2. M. Vincenti, *J. Mass Spectrom.* 1995, **30**: 925-939
3. C. J. Pedersen, *J. Am. Chem. Soc.* 1967, **89**, 2495-2496.
4. J. M. Lehn, J. P. Sauvage and B. Diedrich, *J. Am. Chem. Soc.* 1970, **92**, 2916-2918.
5. . R. Moran, S. Karbach and D. J. Cram, *J. Am. Chem. Soc*. 1982, **104**, 5826-5828.

6. D. J. Cram, S. Karbach, Y. H. Kim, L. Baczynskyj and G. W. Kalleymeyn, *J. Am. Chem. Soc.* 1985, **107**, 2575-2576.
7. L. Seridi and A. Boufelfel , *J. Mol. Liq.* 2011, **158**, 151–158.
8. S. Fanali, *J. Chromatogr. A.* 2000, **875**, 89–122.
9. D. W. Armstrong and U. B. Nair, *Electrophoresis* 1997, **18**, 2331–2342.
10. T. J. Ward and T. M. Oswald, *J. Chromatogr A* 1997, **792**, 309–325.
11. J. Haginaka, *J. Chromatogr*. *A*. 2000**, 875**, 235–254.
12. K. Otsuka and S. Terabe, *J. Chromatogr. A* 2000, **875**, 163–178.
13. E. Anslyn, Modern Physical Organic Chemistry, University Science Books 2006.
14. . B. De Sousa, A. M. L. Denadai, I. S. Lula, J. F. Lopes, H. F. Dos Santos, W. B. De Almeida and R. D. Sinisterra, *Int. J. Pharm.* 2008, **353**, 160–169.
15. J. K. Khedkar, W. Gobre, R. V. Pinjari and S. P. Gejji, *J. Phys. Chem. A*, 2010, **114**, 7725–7732.
16. A. Maheshwari and D. Sharma, *J. Incl. Phenom. Macro.* 2010, **68**, 453–459.
17. M. Jug, N. Mennini, F. Melani, F. Maestrelli and P. Mura, *Chem. Phys. Lett.* 2010, **500**, 347–354.
18. X. H. Wen, Z. Y. Liu and T. Q. Zhu, *Chem. Phys. Lett.* 2005, **405**, 114–117.
19. A. Zoppi, M. A. Quevedo, A. Delrivo and M. R. Longhi, *J. Pharm. Sci.* 2010, **99**, 3166–3176.
20. H. F. Dos Santos, H. A. Duarte, R. D. Sinisterra, S. V. De Melo Mattos, L. F. C. De Oliveira and W. B. De Almeida, *Chem. Phys. Lett.* 2000, *319*, 569–575.
21. W. Snor, E. E. Liedl, P. Weiss Greiler, H. Virnstein and P. Wolschann, *Int. J. Pharm.* 2009, **381**, 146–152.

22. D. J. Barbiric, E. A. Castro and R. H. de Rossi, *J. Mol. Struct. (Theochem)*. 2000, **532**, 171–181.

23. H. A. Dabbagh, M. Zamani and H. Farrokhpour, *Chem. Phys.* 2012, **393**, 86–95.

24. G. J. Chen, S. Su and R. Z. Liu*, J. Phys. Chem. B*, 2002, **106***,* 1570–1575.

25. M. Teranishi, H. Okamoto, K. Takeda, K. Nomura, A. Nakano, R.K. Kalia, P. Vashishta and F. Shimojo, *J. Phys. Chem. B,* 2009, **113**, 1473–1484.

26. J. D. Hartgerink, J. R. Granja, R. A. Milligan and M. R. Ghadiri, *J. Am. Chem. Soc.* 1996, **118**, 43–50.

27. H. W. Tan, W. W. Qu, G. J. Chen and R. Z. Liu, *Chem. Phys. Lett*. 2003, **369**, 556–562.

28. R. Poteau and G. Trinquier, *J. Am. Chem. Soc.* 2005, **127**, 13875–13889.

29. F.Yokoyama, N. Suzuki, M. Haruki, N. Nishi, S. Oishi, N.Fujii, A. Utani, H. K. Kleinman and M. Nomizu, *Biochem.* 2004, **43**, 13590-13597.

30. M. Bagheri, S. Keller and M. Dathe, *Antimicrob. Agents Chemother.* 2011, **55**, 788-797.

31. M. Kracht, H. Rokos, M. Ozel, M. Kowall, G. Pauli and J. Vater, *J. Antibiot.* 1999, **52**, 613-619.

32. S. R. Tendulkar, Y. K. Saikumari, V. Patel, S. Raghotama, T. K. Munshi, P. Balaram and B. B. Chattoo, *J. Appl. Microbiol.* 2007, **103**, 2331-2339.

33. C. Weber, G. Wider, B. von Freyberg, R. Traber, W. Braun, H. Widmer and K. Wuthrich, *Biochem.* 1991, **30**, 6563-6574.

34. G. Trevisan, G. Maldaner, N. A. Velloso, S. Sant'Anna Gda, V. Ilha, C. Velho Gewehr Cde, M. A. Rubin, A. F. Morel and J. Ferreira, *J. Nat. Prod.* 2009, **72**, 608–612.

35. H. Z. Gang, J. F. Liu and B. Z. Mu, *J. Phys. Chem. B* 2010, **114**, 2728–2737.

36. A. Banerjee and A. Yadav, *Appl. Nanosci.* 2012, 1–14.

37. J. Liu, J. Fan, M. Tang and W. Zhou, *J. Phys. Chem. A* 2010, **114**, 2376–2383.

38. R. Vijayaraj, S. Sundar Raman, R. Mahesh Kumar and V. Subramanian *J. Phys. Chem. B.* 2010, **114** 16574–16583.

39. R. Vijayaraj, S. Van Damme and P. Bultinck, *Phys. Chem. Chem. Phys.* 2012, **14**, 15135–15144.

40. P. Zero, F. Plucinski and A. P. Mazurek, *J. Mol. Struct. (Theochem)*.2009, **915** 182–189.

41. R. A. Jishi, R. M. Flores, M. Valderrama, L. Lou and J. Bragin, *J. Phys. Chem.* A 1998, **102**, 9858–9862.

42. H. Zhao, Y. Zhu, M. Tong, J. He, C. Liu and M. Tang, *J. Mol. Model.* 2012, **18**, 851–858.

43. X. Chen, M. Tirado, J. D. Steill, J. Oomens and N. C. Polfer, *J. Mass. Spectrom.* 2011, **46**, 1011-1015.

44. P.Y. Iris Shek, J. Kai-Chi Lau, J. Zhao , J. Grzetic, U. H. Verkerk , J. Oomens, A. C. Hopkinson and K.W. Michael Siu, *Int. J. Mass. Spectrom.* 2012, **316-318**, 199-205.

45. J. S. Klassen and P. l. Kebarle, *J Am. Chem. Soc.* 1997, ***119,*** 6552-6563.

46. T. Yalcin, C. Khouw, I. G. Csizmadia, M. R. Peterson and A. G. Harrison, *J. Am. Soc. Mass Spectrom.* 1995, **6**, 1165.

47. T. Yalcin, I. G. Csizmadia, M. B. Peterson and A. G. Harrison. *J. Am. Soc. Mass Spectrom*. 1996, **7**, 233.

48. S. M. Williams and J. S. Brodbelt, *J. Am. Soc. Mass Spectrom*. 2004, **15**, 1039–1054.

49. K. Schwing, C. Reyheller, A. Schaly, S. Kubik and Ma. Gerhards, *Chem. Phys. Chem.* 2011, **12**, 1981–1988.

50. L. C. M. Ngoka and M. L Gross, *J. Mass. Spectrom.* 2000**, 35***,* 265–276.

51. A. P. Mendham, T. J. Dines, M. J. Snowden, B. Z. Chowdhry and R. Withnall, *J. Raman Spectrosc.* 2009, **40**, 1478–1497.

52. B. T. Ruotolo, C. C. Tate and D. H. Russell, *J. Am. Soc. Mass Spectrom*. 2004, **15**, 870-878.

53. L. C. M. Ngoka and M. L. Gross, *Int. J. Mass Spectrom.* 2000**, 194**, 247–259.

54. C. M. N. Lambert, M. L. Gross and P. L. Toogood, *Int. J. Mass Spectrom.* 1999, **182/183**, 289–298.

55. S. Lin, S. Liehr, B. S. Cooperman and R. J. Cotter, *J. Mass Spectrom.* 2001, **36**, 658–663.

56. N. S. Nagornova, M. Guglielmi, M. Doemer, I. Tavernelli, U. Rothlisberger, T. R. Rizzo and O. V. Boyarkin, *Angew. Chem. Int. Ed.* 2011, **50**, 5383 –5386.

57. L. Zhang, Z. Luo, L. Zhang, L. Jia and L. Wu, *J. Biol. Inorg. Chem.* 2013, **18**,277–286.

58. M. Ngu-Schwemlein, W. Gilbert, K. Askew and S. Schwemlein, *Bio. org. Med. Chem. Lett.* 2008, **16**,5778–5787.

59. F. Shahangi, A. N. Chermahini, H. A. Dabbagh, A. Teimouri and H. Farrokhpour *Comput. Theor. Chem.* 2013, **1020**, 163–169.

60. A. N. Chermahini, M. Rezapour and A. Teimouri, *J. Incl. Phenom. Macro*. 2014, **79**, 205-214.

61. M. Kamiya, T. Tsuneda and K.Hirao, *J. Chem. Phys.* 2002, **117**, 6010-6015.

62. P. J. Stephens, F. J. Devlin, C. F. Chabalowski and M. J. Frisch, *J. Phys. Chem.* 1994, **98**, 11623–11627.

63. T. Yanai, D. P. Tew and N. C. Handy, *Chem. Phys. Lett.* 2004, **393**, 51–57.

64. N. C. Polfer, J. Oomens and R. C. Dunbar, *Chem. Phys. Chem.* 2008, **9**, 579 – 589.

65. C. Colas, S. Bouchonnet, F. Rogalewicz-Gilard, M. Popot and G. Ohanessian, *J. Phys. Chem. A*. 2006, **110**, 7503-7508.

66. T. Marino, N. Russo and M. Toscano, *Inorg. Chem*. 2001, **40**, 6439-6443.

67. A. D. Beck, *J. Chem. Phys.*1993, **98**, 5648-5652.

68. S. F. Boys and F. Bernardi, *Mol. Phys.* 1970, **19**, 553–566.

69. A. E. Reed, R. B. Weinstock and F. Weinhold, *J. Chem. Phys.* 1985, **83**, 735–746.

70. A. E. Reed, L.A. Curtiss and F. Weinhold, *Chem. Rev*. 1988, **88**, 899–926.

71. M. J. Frisch et al., Gaussian 09, Revision B.01, Gaussian, Inc., Wallingford, CT, **2009**.

72. R.F.W. Bader, Atoms in Molecules, A Quantum Theory, International Series of Monographs in Chemistry, vol. 22, Oxford University Press, Oxford, 1990.

73. P.L.A. Popelier, *Coord. Chem. Rev*. 2000, **197**, 169–189.

74. R.F.W. Bader, *Chem. Rev.* 1991, **91**, 893–928.

75. S. De, A. Boda and S.M. Ali, *J. Mol. Struct. (Theochem)*. 2010, **941**, 90–101.

76. S. Kubik and R .Goddard, *Chem. Commun.* 2000, 633–634.

77. G. Praveena and P. Kolandaivel, *J. Mol. Struct. (Theochem)*. 2009, **900**, 96–102.